

Structural and elastic properties of Ge after Kr-ion irradiation at room temperature

R. C. Birtcher and M. H. Grimsditch

Materials Science Division, Argonne National Laboratory, Argonne, Illinois 60439

L. E. McNeil

Department of Physics and Astronomy, University of North Carolina, Chapel Hill, North Carolina 27599-3255

(Received 28 March 1994)

Changes in the elastic properties of Ge induced by room-temperature irradiation with 3.5-MeV Kr ions have been determined and correlated with changes in the microstructure determined by transmission electron microscopy. Elastic-shear-moduli changes were measured by Brillouin scattering, and changes in local atomic arrangement were determined by Raman scattering. Amorphization decreased the elastic shear modulus of Ge by 17%. The fractional decrease was correlated with the amorphous volume fraction with a cross section of $4.5 \pm 0.5 \text{ nm}^2/\text{ion}$. No change was observed in the shear modulus during void formation and growth. The elastic properties of the voided material are described by the Voigt averaging. However, as the voids evolved into a fibrous spongelike microstructure, a second dramatic elastic softening occurs which we attribute to the inability of the fibrous structure to support shear stresses. Raman scattering showed that, once formed, there was no change in the structure of the amorphous material at the atomic scale during void formation and subsequent void coalescence.

INTRODUCTION

Many crystalline materials can be rendered amorphous by a variety of techniques.¹ However, except for ion irradiation, none of these techniques are able to control in a reproducible manner both the rate and degree of the amorphization process. This control allows measurement of changes that occur during the amorphization process. The ultimate aim of this type of investigation is to understand the microscopic nature of the amorphization process. The most severe difficulty in studying irradiation-amorphized samples is that the damage is confined to a relatively thin region ($\approx 1 \mu\text{m}$) near the irradiated surface, requiring measurement techniques that are sensitive to small amounts of material. Based on the behavior of elastic properties during amorphization, Okamoto and Meshii² have suggested that the amorphization process can be described by a generalization of the Lindemann melting criterion in which the critical mean atomic displacement required for melting is replaced by a critical strain required for amorphization. The role of strain generated by defects and chemical disordering has been investigated with molecular dynamics for several ordered alloyed systems.^{3,4} Both chemical disordering and point defects increase the system energy and volume. In some intermetallic systems, chemical disorder is sufficient to induce amorphization, while point defects, i.e., interstitials and vacancies, are required in others.

The energy dependence of amorphization of Ge by Kr ions has been previously determined for thin, approximately 50-nm-thick, specimens as a function of energy by *in situ* transmission electron microscopy (TEM).⁵ Because amorphization of Ge is produced by a single ion,⁶ there is no threshold dose for the onset of amorphization. During 3.5-MeV Kr irradiation, the thin specimen remained in a mixed crystalline and amorphous state until a dose of

$2.0 \times 10^{14} \text{ Kr/cm}^2$, above which electron diffraction spots were no longer detectable and complete amorphization had occurred. Complete amorphization in the above context does not provide a quantitative measure of the limits at which some crystalline material remains. Within experimental uncertainty, between ion energies E_{Kr} of 0.5 and 3.5 MeV the ion dose ϕ_A required for complete amorphization is given by⁵

$$\phi_A (10^{14} \text{ Kr/cm}^2) = 0.55 + 0.43E_{\text{Kr}} (\text{MeV}). \quad (1)$$

The increase in the complete amorphization dose with increasing ion energy reflects a decreasing displacement cross section and a decreasing efficiently to produce damage with increasing ion energy.^{7,8}

In a thick specimen, the dose required for full amorphization is depth dependent, due to the variation of the required amorphization dose with ion energy and due to ion energy loss, straggling, and stopping. Penetration of 3.5-MeV ions into Ge was calculated by the TRIM program.¹⁸ The calculated ion stopping and energy losses were combined with Eq. (1) to estimate the depth dependence of the complete amorphization dose shown in Fig. 1. The 3.5-MeV ions produce inhomogeneous damage along their paths, and averages can present a somewhat misleading picture. Since there is no threshold dose for amorphization, amorphization of a bulk specimen starts at the lowest dose and the specimen will be in a mixed crystalline and amorphous state. Complete amorphization at a depth of $1.2 \mu\text{m}$ below the specimen surface will be achieved after a dose of $1.2 \times 10^{14} \text{ Kr/cm}^2$ and amorphization will progress with increasing ion dose toward both the surface and the interior. The amorphous layer extends to the Ge surface after a dose of $2.0 \times 10^{14} \text{ Kr/cm}^2$ and penetrates to a depth of about $1.7 \mu\text{m}$. The rate of amorphization as a function of depth can be inferred from Fig. 1.

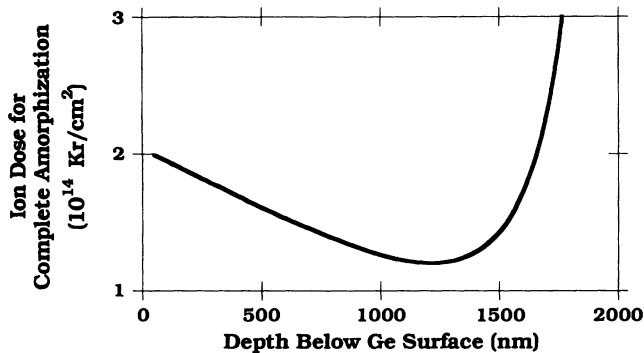


FIG. 1. 3.5-MeV Kr ion dose required for complete amorphization of bulk Ge at room temperature as a function of depth based on measured amorphization doses in thin specimens and TRIM calculation of ion stopping and energy loss.

An extensive discussion of the microstructural evolution observed by transmission electron microscopy has been reported for Ge irradiated at room temperature with 1.5-MeV Kr ions.⁹ At doses greater than 5×10^{14} Kr/cm 2 , voids form in amorphous HGE at room temperature. These voids grow during continued irradiation but do not coalesce, as is found for metals. Instead they repel each other as they grow. As also found in other amorphous materials during irradiation,¹⁰ the material around voids exhibits plastic flow which leads to large deformations. Repulsion between growing voids in Ge leads to the development of a porous spongy structure at an ion dose of 10^{16} Kr/cm 2 . Fully developed, the sponge structure consists of 15–20-nm thick fibers and results in a volume swelling of several hundred percent.

Conversion to the amorphous state is known to produce drastic changes to mechanical properties. The elastic moduli of bulk zirconium silicate (mineral zircon, ZrSiO $_4$) showed a decrease of 70% upon amorphization due to damage produced by naturally occurring radioactive impurities.^{11,12} Brillouin scattering has been used to investigate changes in the shear elastic modulus after ion-beam irradiation in several intermetallic alloys and semiconductors. A large elastic softening preceded amorphization of Zr $_3$ Al,¹³ Nb $_3$ Ir,¹⁴ and FeTi,¹⁵ while the softening was concurrent with amorphization in Si (Ref. 16) and GaAs.¹⁷ The large softening in the intermetallics is believed to be due to chemical disordering that precedes amorphization. The concurrence in the cases of Si and GaAs is a consequence of direct amorphization by individual ions and the resulting mixture of amorphous and crystalline material.

In this work, radiation-induced amorphization of pure Ge has been studied using Brillouin and Raman scattering. We have determined changes in the shear elastic modulus by Brillouin scattering as a function of ion dose through the regimes of amorphization, void formation and growth, and void coalescence into a spongelike framework.

EXPERIMENTAL

Brillouin and Raman scattering measurements were made on a polished bulk Ge single crystal irradiated in a

high-vacuum chamber with 3.5-MeV Kr ions provided by a tandem ion accelerator. Discrete irradiation doses between 10^{12} and 2×10^{16} Kr/cm 2 were made at room temperature inside separate 3-mm-diameter circumscribed areas on the surface. Based on TRIM calculations, almost all implanted Kr ions stop at depths greater than 1.5 μ m, and after our highest Kr dose, only an estimated 135 ppm of Kr ions were retained in the 0.5- μ m-thick surface layer of the specimen that is sampled by Brillouin scattering.

After irradiation the specimen was removed from the ion-beam facility, and Brillouin scattering was used to measure the velocity of the surface waves in each of the different irradiated spots and several unirradiated areas.¹⁴ These measurements employed a single-mode Ar laser, polarized in the scattering plane with approximately 150 mW of power at a wavelength of 514.5 nm. Measurements were made in a backscattering arrangement with the incident and scattered beams 60° from the normal to the specimen surface. The scattered light was frequency analyzed with a scanning 5+2 tandem Fabry-Pérot interferometer. Measured frequency shifts were used to calculate the surface wave velocity. The phonons probed with this technique and in this scattering geometry are surface waves with a wavelength of 297 nm. The frequency of surface waves is determined in principle by the shear elastic constants of the damaged layer and those of the substrate. However, because the surface waves penetrate less than ≈ 0.5 μ m into the material, only the modulus of the irradiated near-surface region is probed. Implanted Kr ions can be neglected because they penetrate to depths far beyond the depth probed by the phonons. Raman scattering experiments, which provide a measure of the density of vibrational states, were recorded on the same samples used for the Brillouin measurements. Spectra were recorded on a double spectrometer using 100 mW of 476-nm radiation.

RESULTS AND DISCUSSION

A. Brillouin scattering

Creation of an amorphous volume fraction in Ge leads to a decrease or softening of the average elastic shear modulus and a consequent reduction in the velocity of the surface modes. Figure 2 shows the dose dependence of the velocity of surface waves on a $\langle 111 \rangle$ face of Ge. Values plotted at a dose of 10^{11} Kr/cm 2 are for unirradiated spots on the Ge surface. The data in Fig. 2 show two sharp decreases with increasing ion dose. The first decrease of the surface wave velocity starting from the lowest doses coincides with the appearance of diffuse electron scattering during *in situ* transmission electron microscopy experiment,^{5,9} indicating the presence of an amorphous volume fraction. The second decrease occurs at doses where a spongelike structure is observed.

The shear velocity is a function of the material density and its shear elastic modulus. Considering the irradiated surface layer sampled by Brillouin scattering to be a composite of crystalline and amorphous Ge and using Voigt's approximation, which assumes continuity of displacements at the interfaces between constituents, for the average elastic constant,¹⁹ the shear wave velocity is given by

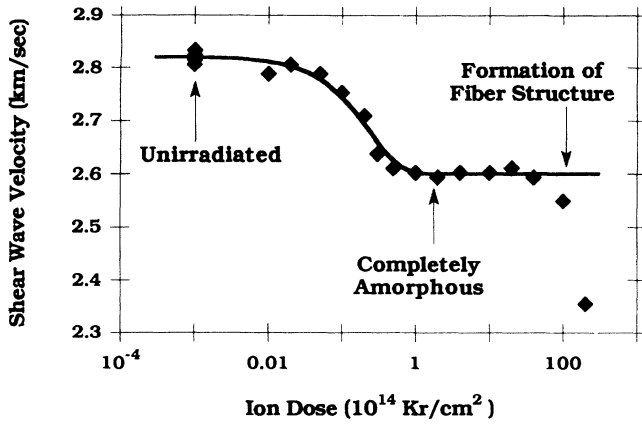


FIG. 2. Shear wave velocity of Ge irradiated at room temperature with 3.5-MeV Kr ions as measured by Brillouin scattering. For convenience, values from unirradiated Ge are plotted at a dose of 10^{11} Kr/cm 2 . The symbols are experimental points, and the line is a fit according to Eqs. (3) and (4).

$$V^2 = \frac{f_x C_x + f_a C_a}{f_x \rho_x + f_a \rho_a} \quad (2)$$

where the subscript x refers to crystal material, the subscript a refers to amorphous material; and f_i is the volume fraction, C_i is the shear modulus, and ρ_i is the density of the i th component in the composite. Since at lower doses we see no void formation, $f_a = 1 - f_x$. The shear velocity will vary between the unirradiated crystal value of $\sqrt{C_x/\rho_x}$ and the value for amorphous Ge of $\sqrt{C_a/\rho_a}$. With the approximation that the difference in density is small, the shear velocity for the composite is given by

$$V^2 = \frac{C_a}{\rho_a} + \left[\frac{C_x}{\rho_x} - \frac{C_a}{\rho_a} \right] f_x \quad (3)$$

Since the density of Ge decreases by $\approx 3\%$ on amorphization, Eq. (3) should be a good approximation. We note that, if the changes in both C and ρ are small, Eq. (3) is independent of having used the Voigt average, and the same expression is obtained if the Reuss average is assumed.²⁰

Direct amorphization by individual ions results in the volume fraction of crystalline material decreasing as $f_x = e^{-\sigma\phi}$, where ϕ is the ion dose and σ is the cross section for amorphization. The first decrease in Fig. 2 (up to a dose of 2×10^{15} Kr/cm 2) has been fitted assuming this form for f_x and using Eq. (3). The fit yields a value for σ of 4.5 ± 0.3 nm 2 for 3.5-MeV Kr ions. Based on this value for σ , the fraction of crystalline material remaining after complete amorphization, defined as the disappearance of all diffraction spots in TEM, is 1×10^{-4} .

The interpretation given above is somewhat oversimplified since it ignores the fact that the sensitivity of the Brillouin measurements changes with depth and that the production of amorphous material is depth dependent. The amorphization cross section varies with ion energy, and in a thick specimen both the ion energy

and flux vary with depth from the surface. The Kr-ion energy variation with depth and ion stopping were calculated with the TRIM code,¹⁸ and variation of the complete amorphization dose with energy has been taken from the measured variation in thin specimens described by Eq. (1). Brillouin scattering has a depth-dependent sensitivity to the shear constant that decreases with an exponential length constant related to the phonon wavelength. In this work that length constant is 300 nm. In a more complete calculation, the cross section for amorphization was determined by fitting the first decrease shown in Fig. 2 using Eq. (3) along with the depth dependencies of the amorphization dose and sensitivity of Brillouin scattering. For the purpose of calculating the shear velocity, the specimen was divided into 50-nm-thick layers and the volume fraction amorphized with the ion dose was summed over the 500-nm surface layer with the contribution to the Brillouin scattering from each layer exponentially damped with a 300-nm length constant. The average cross section for amorphization determined by the fit shown in Fig. 2 is 4.5 ± 0.5 nm 2 . This value is, within uncertainty, the same as that derived under the assumptions of uniform damage and measurement sensitivity. This is because of the small variation of the amorphization cross section with ion energy at the ion energy used in this experiment.

The above value of σ can be compared with those for other materials which have been derived with the assumption that there was no depth dependence to amorphization: a value of 0.125 nm 2 was found for Si irradiated with 1.8-MeV Kr ions at room temperature while after liquid-nitrogen-temperature irradiation and anneal to room temperature the value was approximately 1 nm 2 .¹⁶ A value of 0.82 nm 2 was found for GaAs irradiated with 1.5-MeV Kr ions at room temperature.¹⁷ Defect recovery during irradiation of GaAs and Si increases the ion dose required for amorphization, decreasing the effective values of σ . Because lower ion energies were used, damage gradients in Si and GaAs produced by energy loss and ion stopping will affect the extracted values of σ .

Based on calculations using TRIM,¹⁸ 3.5-MeV Kr ions produce an average of 12 vacancies/nm in the 500-nm-thick region samples by Brillouin scattering. This yields an average value of approximately 16 amorphized lattice sites per vacancy in Ge. For Si the estimated values of σ correspond to 0.23 and 2.1 amorphized lattice sites per vacancy at room temperature and liquid-nitrogen temperature, respectively. For GaAs, σ corresponds to 2.3 amorphized lattice sites per vacancy. The values for Si and GaAs are lowered by defect recovery.

Over the dose range between 0.25×10^{15} and 5×10^{15} Kr/cm 2 , there was no change in the surface wave velocity measured by Brillouin scattering in spite of the formation and growth of voids in the amorphous Ge. Considering the surface layer sampled by Brillouin scattering to be a composite of amorphous Ge and voids and using Voigt's approximation for the average elastic constant, the surface wave velocity is given by Eq. (2) where the subscript x must now be replaced by a V representing the voids. Since the voids contain at most a few Kr atoms, $C_V = \rho_V = 0$, and Eq. (1) simplifies to

$$V = \sqrt{C_a / \rho_a} . \quad (4)$$

It should be noted that Eq. (4) depends only on the choice of the Voigt average for the elastic constants. We recall that the Voigt average is based on the assumption that the strain in the two constituents of the material is the same; for an isolated void in a solid matrix this is a reasonable assumption. Because Eq. (4) is independent of the fraction of the material occupied by voids, Brillouin scattering is insensitive to void formation provided the elastic stiffness of the surrounding material is unchanged by the structural arrangement. Equation (4) accurately describes the results shown in Fig. 2 over two decades of ion doses during which void growth occurs. At ion doses above 5×10^{15} Kr/cm², Eq. (4) clearly no longer describes the observed behavior in spite of the fact that the structure of amorphous Ge at the atomic level does not change appreciably above this dose (see next section). Since the only other assumption in deriving Eq. (4) is the choice of the Voigt averaging procedure, we conclude that this form of averaging is not appropriate when the voids become interconnected. Since the correct averaging procedure for such a heterogeneous material is still an unsolved problem, a discussion of our results in terms of the various models and approximations proposed adds little to an understanding of the experimental results. We note, for example, that if the Reuss average were used, the resulting velocity would be zero: also in clear disagreement with experiment.

From a phenomenological standpoint the second sharp decrease observed in Fig. 2, starting at about a dose of 10^{16} Kr/cm², coincides with the appearance of the fibrous spongy microstructure observed in TEM.⁹ This microstructural change is responsible for a large amount of swelling and a decrease in density of the surface layer. It has been estimated⁹ that the swelling amounts to several hundred percent, corresponding to a macroscopic density decrease to a few percent of its initial value. As argued above (using the Voigt average), this change in average macroscopic density should not by itself change the shear velocity measured by Brillouin scattering. Instead, the observed decrease in the shear velocity arises from the topological changes of the voided regions. A quantitative understanding of this effect will require extensive modeling.

In addition to the decrease in shear velocity observed at ion doses above 10^{16} Kr/cm², the nature of the Brillouin spectra change. Figure 3 shows Brillouin spectra recorded on samples irradiated to 1 and 2×10^{16} Kr/cm², respectively. At the lower dose, a single peak characteristic of a surface wave is observed; at the higher dose a double-peak structure develops. Figure 4 shows the velocity of the two modes as a function of the wave-vector component along the surface. (The change in wave vector was achieved by varying the angle of incidence in the Brillouin experiments.) The velocity of the lower-frequency mode is consistent with the expected dependence for surface (also known as Rayleigh) waves on a thin-film-substrate combination. The wave-vector dependence of the upper mode is reminiscent of that of higher-order (Sezawa) surface waves also expected for a

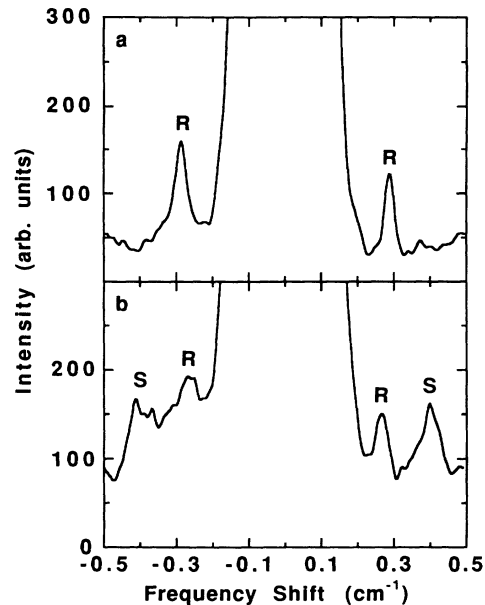


FIG. 3. Brillouin spectra from Ge irradiated at room temperature with (a) 1 and (b) 2×10^{16} Kr/cm². The peaks labeled R are the usual surface (Rayleigh) waves; the origin of the peaks labeled S is unknown.

thin film on a substrate.²¹ Because these modes result from “reflections” at the interface and free surface they can only exist for velocities lower than the substrate shear velocity. (If this condition is not met the waves do not “reflect” at the film-substrate interface.) Since the measured velocity is greater than the shear velocity in the substrate, the interpretation of the additional feature as a Sezawa mode is suspect. A second possible explanation is that the optical properties of the porous Ge film are such that it allows coupling to bulk waves propagating perpendicular to the surface. If this were the case the measured frequency shift should be independent of the component of the wave vector parallel to the surface, q_{\parallel} , and the velocity, calculated as $\Delta\omega/q_{\parallel}$, should scale as $1/q_{\parallel}$. This is also in disagreement with our observations. We believe that the most reasonable explanation is that this mode is

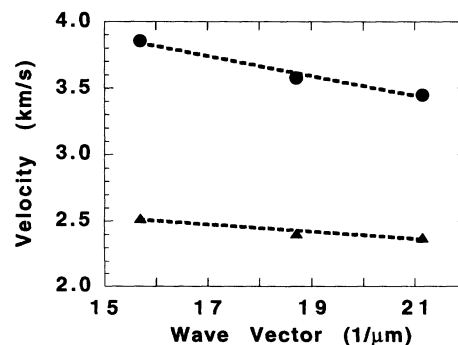


FIG. 4. Wave-vector dependence of the velocity of the two modes observed in Fig. 3(b). Triangles (circles) correspond to the lower (upper) mode in Fig. 3(b). The lines are guides to the eye.

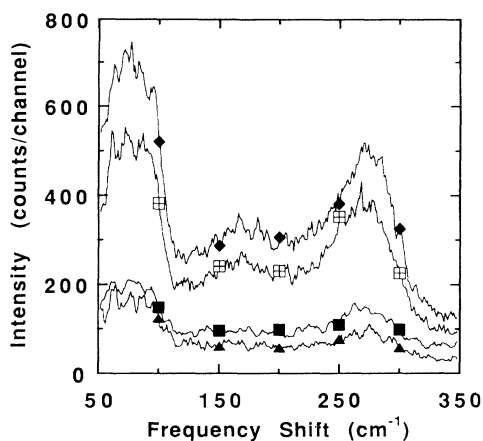


FIG. 5. Raman spectra from Ge irradiated at room temperature with 0.01 (solid squares), 0.2 (solid triangles), 2 (diamonds), and 3 (open squares) $\times 10^{16}$ Kr/cm².

a Sezawa-like surface wave which exists as a “resonance”²² with the substrate continuum of excitations. Such resonances have been observed and could arise in this case due to the large impedance mismatch between the spongy film and the substrate.

B. Raman scattering

Figure 5 shows Raman spectra recorded from samples irradiated with 0.01, 0.2, 2, and 3×10^{16} Kr/cm². The spectral features observed in Fig. 5 are typical of those of “ordinary” *a*-Ge produced by sputtering techniques.²³ The most significant feature of Fig. 5 is that the spectral features are not affected by the formation of voids or by the formation of the spongelike structure. Since Raman spectra reflect the density of vibrational states in the material, our spectra imply that, at the microscopic level, there is no structural change when the material undergoes the second pronounced elastic softening. The moduli changes occurring at these does must therefore be related to the connectivity of the structure and not to a structural rearrangement at the atomic level.

Another feature of the spectra in Fig. 5 is that the Raman spectra from the fibrous structure (diamonds and open squares) are considerably more intense. Even though a comparison of intensities between two spectra is fraught with possible errors, the intensity changes are large enough that it is clear that the differences produced

by the fibrous structure are real. We lack an explanation for the observed increase. Speculations as to its origins are that (i) the fibrous structure is optically more transparent so that a larger volume of sample is probed; (ii) the fibrous structure exposes a larger surface area to the incident laser beam; or (iii) changes in the electron structure of the material lead to a resonant enhancement of the scattering process. A definitive explanation of this observation clearly requires further work. We believe that an ellipsometric determination of the optical properties of the surface layer could provide valuable insight into the origin of the phenomenon.

CONCLUSIONS

The elastic properties of Ge, like those of Si and GaAs, exhibit a softening with increasing degree of amorphization during ion irradiation. This is in marked contrast with the behavior of intermetallic compounds such as Zr₃Al and Nb₃Ir in which the softening precedes amorphization. Direct amorphization by single ions in the semiconductors is responsible for the concurrent decrease of the elastic shear modulus with amorphization, while chemical disordering before amorphization in the intermetallics is responsible for softening of the shear modulus before onset of amorphization. Based on fitting the decrease in the shear velocity, the average cross section of amorphization is 4.5 ± 0.5 nm², and approximately 16 lattice sites are amorphized for each vacancy produced in Ge by 3.5-MeV Kr ions. This indicates that complete amorphization observed by TEM occurs when the volume fraction of crystalline material decreases to 1×10^{-4} . The formation and growth of voids in amorphous Ge do not affect the shear modulus. This implies that the elastic properties of the voided material are described by the Voigt average. This description remains valid until the voids coalesce to form a fibrous spongy structure. When this occurs, a substantial additional softening of the shear modulus is observed but the microscopic nature of the atomic bonding, as determined by Raman scattering, is unchanged.

ACKNOWLEDGMENTS

We would like to thank B. J. Kestel for specimen preparation and P. M. Baldo for help with the ion irradiations. This work was supported by the U.S. Department of Energy, BES–Materials Sciences, under Contract No. W-31-109-Eng-38.

¹R. W. Cahn and W. L. Johnson, *J. Mater. Res.* **1**, 724 (1986).

²P. R. Okamoto and M. Meshii, in *Science of Advanced Materials*, edited by H. Wiedersich and M. Meshii (American Society for Metals, Metals Park, OH, 1990).

³M. J. Sabochick and N. Q. Lam, *Phys. Rev. B* **43**, 5243 (1991).

⁴N. Q. Lam, P. R. Okamoto, R. Devanathan, and M. Meshii, in *Statics and Dynamics of Alloy Phase Formation*, Vol. 319 of NATO Advanced Study Institute, Series B: Physics, edited by P. E. A. Turchi and A. Gonis (Plenum, New York, 1992).

⁵R. C. Birtcher, in *Beam-Solid Interactions: Fundamentals and*

Applications, edited by M. A. Nastasi, L. R. Harriott, N. Herbots, and R. S. Averback, MRS Symposia Proceedings No. 279 (Materials Research Society, Pittsburgh, 1993), p. 129.

⁶L. W. Howe and M. H. Rainville, *Nucl. Instrum. Methods Phys. Res. Sect. B* **19/20**, 61 (1987).

⁷R. S. Averback, R. Benedek, and K. L. Merkle, *Phys. Rev. B* **18**, 4156 (1978).

⁸J. H. Kinney, M. W. Guinan, and Z. A. Munir, *J. Nucl. Mater.* **122/123**, 1028 (1984).

⁹L. M. Wang and R. C. Birtcher, *Philos. Mag. A* **64**, 1209

- (1991).
- ¹⁰S. Klaumünzer, C. Li, S. Löffler, M. Rammensee, G. Schumacher, and H. Ch. Neitzert, *Radiat. Eff. Defects Solids* **108**, 131 (1989).
- ¹¹H. Özkan, *J. Appl. Phys.* **47**, 4772 (1976).
- ¹²B. C. Chakoumakos, W. C. Oliver, G. R. Lumpkin, and R. C. Ewing, *Radiat. Eff. Defects Solids* **118**, 393 (1991).
- ¹³L. E. Rehn, P. R. Okamoto, J. Pearson, R. Bradra, and M. Grimsditch, *Phys. Rev. Lett.* **59**, 2987 (1987).
- ¹⁴M. Grimsditch, K. E. Gray, R. Bradra, R. T. Kampwirth, and L. E. Rehn, *Phys. Rev. B* **35**, 883 (1987).
- ¹⁵J. Koike, P. R. Okamoto, L. E. Rehn, R. Bradra, and M. H. Grimsditch, in *Beam-Solid Interactions: Physical Phenomena*, edited by J. A. Knapp, P. Borgesen, and R. A. Zuhr, MRS Symposia Proceedings No. 157 (Materials Research Society, Pittsburgh, 1990), p. 777.
- ¹⁶R. Bhadra, J. Pearson, P. Okamoto, L. Rehn, and M. Grimsditch, *Phys. Rev. B* **38**, 12 656 (1988).
- ¹⁷R. P. Sharma, R. Bhadra, L. E. Rehn, P. M. Baldo, and M. Grimsditch, *J. Appl. Phys.* **66**, 152 (1989).
- ¹⁸J. J. F. Ziegler, J. P. Biersack, and U. Littlemark, *The Stopping Range of Ions in Solids* (Pergamon, New York, 1985).
- ¹⁹W. Voigt, in *Lehrbuch der Krystallophysik* (B. G. Teuber, Leipzig, 1928), p. 962.
- ²⁰A. Reuss, *Z. Angew. Math. Mech.* **9**, 49 (1929).
- ²¹K. Sezawa and K. Kanai, *Bull. Earthquake Res. Inst. (Tokyo)* **13**, 471 (1935).
- ²²R. E. Camley and F. Nizzoli, *J. Phys. C* **18**, 4795 (1985).
- ²³D. Bermejo and M. Cardona, *J. Non Cryst. Solids* **32**, 421 (1979).